Proceedings of Ninth World Conference on Earthquake Engineering
August 2-9, 1988, Tokyo-Kyoto, JAPAN (Vol.II)

3-7-7

DISTRIBUTION OF PHASE DIFFERENCES IN RELATION TO THE EARTHQUAKE MAGNITUDE, DISTANCE TO THE FAULT AND LOCAL SOIL CONDITIONS

Taketsugu YOKOYAMA, Nikolaos THEOFANOPOULOS
and Makoto WATABE

Department of Architecture, Tokyo Metropolitan University,
Fukazawa Setagaya-ku, Tokyo, Japan

SUMMARY

A method for generation of earthquake motions will be presented in this paper. The earthquake motions are generated by superposition of sinusoidal waves with a set of phase angles which depends on earthquake magnitude, distance to the fault and local soil conditions. That set of phase gives to the synthetic waves the information on non-stationarity corresponding to the envelope function. By the use of this method far-field earthquake motions can be satisfactorily simulated.

INTRODUCTION

There are a lot of cases of seismic design where the generation of input earthquake motions is necessary. This problem has been reported by many authors in various ways. In this paper a new method for the generation of synthetic earthquake motions will be described.

The earthquake ground motions are non-stationary in both amplitude and frequency contents, and stochastically quite random. Through the conversion of them into frequency domain, those non-stationarities are reflected into phase components, and not into amplitude components. Therefore, phase components in frequency domain should contain all information about the non-stationarity of the earthquake ground motions. It has been found (Ref. 1, 2, 3) that the distribution of the difference of Fourier phase angles for a recorded earthquake ground motion is highly correlated to its envelop shape. Based upon this fact and examining the phase difference distribution of many accelerograms, it has been correlated to the earthquake magnitude, the distance to the fault and the local soil conditions. Through this way, after deciding the magnitude and the distance of a future earthquake and the soil condition of the site under consideration, an averaged phase difference distribution can be calculated from the regression analysis. The original Fourier amplitudes could be obtained by considering the zero damping velocity response spectrum. Considering both Fourier amplitudes and phase angles, earthquake motions then can be easily generated. The response spectrum of the motions approaches to the target one after repeated corrections of the Fourier amplitudes.

METHOD

Phase Difference Distribution A digitized earthquake motion record a(t) can

be expanded into Fourier series as follows;

$$a(t) = \sum_{k=0}^{N/2} A_k \cos\left(\frac{2\pi}{T_k} t + \Phi_k\right) \tag{1}$$

where A_k is the Fourier amplitude, T_k the period and Φ_k the phase angle. The characteristics of non-stationarity of recorded earthquake ground motions can be expressed by the distribution of the phase difference $\Delta\Phi_k$, which are given by

$$\Delta\Phi_k = \Phi_{k+1} - \Phi_k \tag{2}$$

where $\Delta\Phi_k$ is defined in the interval of $(-2\pi, 0)$.

The phase difference range of $(-2\pi, 0)$ was divided into 36 equal intervals and the relative frequency for each interval was calculated. The distribution of phase differences is quite similar to the envelope of the original record. This fact may be visualized more clearly if the axis of time from 0 to T_d (total duration) and the axis of the phase difference distribution from 0 to -2π are scaled to the same length as shown in Fig. 1.

The characteristics of the phase differences of 3-dimensional earthquake ground motions obtained in Japan, U.S.A. and Greece were analyzed. These accelerograms were obtained due to the earthquakes with magnitudes between 4.5 and 7.9 and with distances to the fault between 0.1 and 240km. The scattergram of magnitudes and distances to the fault of these earthquakes shown in Fig. 2. Only the horizontal components of the data base were transformed to the principal axes. Principal axes are defined as the axes along which the components of earthquake ground motions have maximum and minimum values and covariances approximately equal to zero (Ref. 4). Only the frequency range between the cut-off frequencies of the band-pass filter used during the correction procedures of the earthquake motions was considered. In order to ensure uniform total duration for records at the same range of magnitude, distance to the fault and local soil conditions and obtain better results at the regression analysis, the low amplitude parts at the beginning and at the end of record have been cut-off. The end of the strong motion (T_{end}) was taken equal to

$$T_{end} = T_d - T_l \tag{3}$$

where T_l is the duration of the low amplitude part at the beginning of accelerogram defined from the regression relationships given by Theofanopoulos et al. (Ref. 5). Due to this assumption, some of the records were expanded by adding tailing zeros and the rest of them were shortened to assure the uniformity of phase difference distribution results.

Regression Analyses Weighted regression analyses (Ref. 6) of the phase difference distributions separately for the major, intermediate and vertical axis were conducted at the 36 different intervals of $\Delta\Phi_k$. The mathematical model was selected on the basis of simplicity and fundamental physical arguments that lead to the basic functional dependence of the relative frequency (value of the probability density function for each interval) on the independent variables, such as magnitude (M), distance to the fault (X) and local soil conditions (S). It can be expressed by the following equation;

$$R(\Delta\Phi_i, j) = A(\Delta\Phi_i, j) + B(\Delta\Phi_i, j)M + C(\Delta\Phi_i, j)X + D(\Delta\Phi_i, j)S \qquad i=1,\cdots,36 \text{ and } j=1,2,3 \tag{4}$$

where j=1, 2, 3 for major, intermediate and vertical axis respectively, S=0, 1, 2 for hard, intermediate and soft soil respectively, $R(\Delta\Phi_i, j)$ is the relative

frequency as a function of phase difference $\Delta\Phi_i$, $A(\Delta\Phi_i,j)$, $B(\Delta\Phi_i,j)$, $C(\Delta\Phi_i,j)$ and $D(\Delta\Phi_i,j)$ are the regression coefficients. The resulted phase difference distributions for M=6.0, X=5km, S=2 (CASE 1), M=7.0, X=50km, S=1 (CASE 2) and M=8.0, X=100km, S=0 (CASE 3) are shown in Fig. 3. The resulted values of A, B, C, D for all axes are shown in Table 1 and are plotted in relation to the phase difference $\Delta\Phi_i$ in Fig. 4.

Sub-Distribution The dependence of the phase difference distribution on the frequency was also analyzed at certain ranges of frequencies as shown in Fig. 5. From this figure it can be observed that the phase difference distribution may be different at different ranges of frequencies. The non-uniformity of the phase difference distribution in relation to the frequency may be due to the source characteristics, to delayed arrivals of body waves, or to the influence of the local soil conditions. The relative frequency of the phase difference distribution at the predominant frequency range is zero or approximately zero in the range of $(-2\pi, -\pi)$. In this case the relative frequency becomes high at narrow band of phase differences and vanishes at the rest of them. At frequencies lower than the predominant frequency range, the phase difference distribution seems to be uniform.

Having in mind all these considerations,the phase difference distribution which can be calculated from the derived regression relationships was divided into various sub-distributions for the various ranges of frequencies. In order to accomplish a subdivision, the distribution extent at the predominant frequencies was limited at approximately the range of $(-\pi, 0)$. The distribution for frequencies lower than the predominant frequency range was assumed to be relatively uniform in the range of $(-2\pi, 0)$, keeping the general shape of the distribution derived from the relationships. In the case of hard soil conditions, the distribution for frequencies higher than the predominant was kept similar to the obtained one from the relationships. In the case of soft soil conditions a gradual increasing of the absolute mean value of the distribution has been adopted. The phase differences in each sub-distribution were arranged randomly.

Synthetic Earthquake Motion The phase differences for all axes of earthquake motion can be obtained by the described procedure. Assuming that the initial value of phase angles is equal to zero and taking into account the Eq. (2), the phase angles over the interval $(0, 2\pi)$ can be calculated. Then design response spectra for hard soil which are proposed by Ohsaki et al. (Ref. 7) for magnitude 8.0, distance to the fault 100km have been set. The spectrum at the major axis as multiplied by 1.15 in order to take into account the orthogonality effects. The spectrum of the intermediate and vertical axes were taken equal to 90% and 50% of those of the major axis. By Eq. (1) far-field synthetic earthquake motions along 3-axes were generated, which are shown in Fig. 6. It can be observed a good fitting of the target to the synthetically generated response spectra, as well as, with realistic peak acceleration and duration time.

CONCLUSIONS

A method for generation of synthetic earthquake motions was presented in this paper. The non-stationarity of the earthquake ground motion was obtained through the use of an evolutionary phase difference distribution with different probability density function for different frequency ranges. The resulting synthetic earthquake motions have a shape that depends on the magnitude, distance to the fault and the local soil conditions. By this method, non-stationarity characteristics of the earthquake ground motions can be obtained directly without multiplying a stationary motion by deterministic intensity functions.

ACKNOWLEDGMENT

Authors wish to express their appreciation to Drs. Noda and Kurata of Port and Harbor Research Institute, Ministry of Transport for their permission to use a set of 117 components of Japanese strong motion records.

REFERENCES

1. Ohsaki, Y., "On the Significance of Phase Content in Earthquake Ground Motions", Earthquake Engineering and Structural Dynamics, Vol.7, pp.427-439, (1979).
2. Matsukawa, K., Watabe, M., Theofanopoulos, N., and Tohdo, M., "Phase Characteristics of Earthquake Ground Motions and Those Applications to Synthetic Ones", Transaction of the 9th International Conference on Structural Mechanics in Reactor Technology (SMiRT), Vol.K1, pp.43-48, (1987).
3. Theofanopoulos, N. and Dan, K., "Generation of Input Earthquake Motions for Disaster Countermeasures", Proceedings of the International Symposium on Earthquake Countermeasures, Beijing, China, (1988).
4. Penzien, J., Watabe, M., "Characteristics of 3-Dimensional Earthquake Ground Motions", Earthquake Engineering and Structural Dynamics, Vol.40, No.2, pp.365-373, (1975).
5. Theofanopoulos, N., Watabe, M. and Matsukawa, K., "Strong Motion Duration and Intensity Function", Transaction of the 9th International Conference on Structural Mechanics in Reactor Technology (SMiRT), Vol.K1, pp.31-36, (1987).
6. Theofanopoulos, N., Feng, D. and Tselentis, G., "A New Weighted Scheme of Data in Regression Analysis and Examples of Its Application", Proceedings of the International Seminar on Seismic Zonation, Guangzhou, China, (1987).
7. Ohsaki, Y. et al., "Design Spectra for Stiff Structures on Rock", Proceeding of the 2nd International Conference on Microzonation, Vol.3, (1978).

Table 1 Regression Coefficient Results

$\Delta\Phi_i$	MAJOR AXIS				INTERMEDIATE AXIS				VERTICAL AXIS			
(rad)	$A(\Delta\Phi_i,1)$	$B(\Delta\Phi_i,1)$	$C(\Delta\Phi_i,1)$	$D(\Delta\Phi_i,1)$	$A(\Delta\Phi_i,2)$	$B(\Delta\Phi_i,2)$	$C(\Delta\Phi_i,2)$	$D(\Delta\Phi_i,2)$	$A(\Delta\Phi_i,3)$	$B(\Delta\Phi_i,3)$	$C(\Delta\Phi_i,3)$	$D(\Delta\Phi_i,3)$
-0.09	0.81789E-01	-0.71340E-02	-0.39696E-04	0.75970E-02	0.91709E-01	-0.88743E-02	-0.31007E-04	0.95298E-02	0.11126E+00	-0.10349E-01	-0.66109E-04	0.16572E-01
-0.26	0.16054E+00	-0.12198E-01	-0.15250E-03	-0.60177E-03	0.16864E+00	-0.12768E-01	-0.16888E-03	-0.17391E-02	0.17961E+00	-0.10940E-01	-0.20982E-03	0.46806E-03
-0.44	0.22847E+00	-0.18322E-01	-0.18675E-03	0.12907E-02	0.23296E+00	-0.18079E-01	-0.21116E-03	0.48849E-03	0.21905E+00	-0.15389E-01	-0.18970E-03	0.62835E-02
-0.61	0.19610E+00	-0.13382E-01	-0.15795E-03	0.81585E-02	0.18868E+00	-0.12610E-01	-0.15508E-03	0.53461E-02	0.18103E+00	-0.11355E-01	-0.15399E-03	0.73622E-02
-0.79	0.12270E+00	-0.46337E-02	-0.14370E-03	0.81722E-02	0.10138E+00	-0.15709E-02	-0.14164E-03	0.33546E-02	0.84904E-01	0.12235E-02	-0.12274E-03	0.36196E-02
-0.96	0.31469E-01	0.82328E-02	-0.12898E-03	0.11791E-02	0.40522E-01	0.67789E-02	-0.12411E-03	-0.30967E-02	0.24014E-01	0.84918E-02	-0.75727E-04	-0.13199E-02
-1.13	-0.10844E-01	0.14096E-01	-0.10449E-03	-0.54689E-02	0.64996E-02	0.11502E-01	-0.87145E-04	-0.58712E-02	-0.19830E-01	0.14369E-01	-0.56464E-04	-0.84253E-02
-1.31	-0.12452E-01	0.13647E-01	-0.58343E-04	-0.10280E-01	-0.21323E-01	0.15159E-01	-0.65413E-04	-0.91963E-02	-0.12587E-01	0.10560E-01	0.35748E-05	-0.85544E-02
-1.48	-0.27287E-01	0.14912E-01	-0.50285E-04	-0.10932E-01	-0.18674E-01	0.12445E-01	-0.34881E-04	-0.57981E-02	-0.14986E-01	0.92859E-02	0.20434E-04	-0.67407E-02
-1.66	-0.19016E-01	0.11090E-01	-0.89689E-05	-0.71784E-02	-0.70261E-02	0.84643E-02	-0.42420E-05	-0.43234E-02	-0.10416E-01	0.70768E-02	0.20847E-04	-0.41179E-02
-1.83	-0.13446E-01	0.79837E-02	0.19488E-04	-0.43685E-02	-0.16274E-01	0.85523E-02	0.11196E-04	-0.31513E-02	-0.78164E-02	0.55790E-02	0.27306E-04	-0.36552E-02
-2.01	-0.20741E-01	0.79410E-02	0.23200E-04	-0.26462E-02	-0.16409E-01	0.70203E-02	0.25333E-04	-0.19858E-02	-0.42206E-02	0.37649E-02	0.53691E-04	-0.95052E-03
-2.18	-0.12968E-01	0.55858E-02	0.48431E-04	-0.11459E-02	-0.19783E-01	0.63836E-02	0.39719E-04	-0.61126E-05	-0.57231E-02	0.32471E-02	0.45479E-04	0.10462E-02
-2.36	-0.70502E-02	0.34760E-02	0.51370E-04	-0.21411E-03	-0.12702E-01	0.43412E-02	0.44518E-04	0.11467E-02	0.44825E-02	0.10398E-02	0.57452E-04	0.19079E-02
-2.53	0.49476E-03	0.12970E-02	0.73643E-04	0.18836E-02	-0.47515E-02	0.19747E-02	0.65066E-04	0.43345E-02	-0.94785E-03	0.14276E-02	0.53765E-04	0.18437E-02
-2.70	0.24834E-02	0.46820E-03	0.68885E-04	0.29082E-02	0.32129E-02	0.43203E-03	0.64706E-04	0.31869E-02	0.41562E-02	0.34417E-03	0.48696E-04	0.14464E-02
-2.88	0.13777E-01	-0.17850E-02	0.72534E-04	0.35594E-02	0.57220E-02	-0.33828E-03	0.62692E-04	0.40832E-02	0.61540E-02	-0.35734E-03	0.50702E-04	0.19313E-02
-3.05	0.10883E-01	-0.13271E-02	0.60318E-04	0.31323E-02	0.85059E-02	-0.64946E-03	0.51185E-04	0.26455E-02	0.13713E-01	-0.12066E-02	0.37152E-04	0.75574E-03
-3.23	0.12568E-01	-0.18577E-02	0.53133E-04	0.37034E-02	0.21620E-01	-0.32872E-02	0.76928E-04	0.37584E-02	0.86096E-02	-0.57071E-03	0.27722E-04	0.13844E-02
-3.40	0.12601E-01	-0.18889E-02	0.48615E-04	0.36118E-02	0.15975E-01	-0.25816E-02	0.62700E-04	0.40393E-02	0.87944E-02	-0.73258E-03	0.31560E-04	0.12922E-02
-3.58	0.15426E-01	-0.21999E-02	0.45685E-04	0.26704E-02	0.92734E-02	-0.11475E-02	0.41331E-04	0.27786E-02	0.46193E-02	-0.25595E-03	0.27282E-04	0.17032E-02
-3.75	0.12095E-01	-0.17321E-02	0.38791E-04	0.22269E-02	0.15439E-01	-0.22702E-02	0.38841E-04	0.25087E-02	0.13535E-01	-0.17166E-02	0.29390E-04	0.14621E-02
-3.93	0.14459E-01	-0.22139E-02	0.31953E-04	0.26613E-02	0.11630E-01	-0.15175E-02	0.28494E-04	0.23225E-02	0.84856E-02	-0.81283E-03	0.19726E-04	0.62920E-03
-4.10	0.11248E-01	-0.14733E-02	0.22127E-04	0.16579E-02	0.87328E-02	-0.11809E-02	0.26859E-04	0.24571E-02	0.80862E-02	-0.81446E-03	0.21754E-04	0.91687E-03
-4.28	0.95314E-02	-0.11771E-02	0.22363E-04	0.15197E-02	0.87130E-02	-0.10722E-02	0.24831E-04	0.13780E-02	0.10773E-01	-0.12658E-02	0.19193E-04	0.11856E-02
-4.45	0.12065E-01	-0.14788E-02	0.20655E-04	0.93843E-03	0.10196E-01	-0.10642E-02	0.16786E-04	0.57794E-03	0.63509E-02	-0.62124E-03	0.18110E-04	0.13170E-02
-4.63	0.13423E-01	-0.16802E-02	0.20226E-04	0.71911E-03	0.96697E-02	-0.10455E-02	0.17950E-04	0.87343E-03	0.11734E-01	-0.12407E-02	0.13381E-04	0.38322E-03
-4.80	0.11182E-01	-0.14229E-02	0.18693E-04	0.13900E-02	0.80870E-02	-0.69447E-03	0.13381E-04	0.61949E-03	0.11249E-01	-0.12112E-02	0.15493E-04	0.93620E-03
-4.97	0.11089E-01	-0.11921E-02	0.10000E-04	0.10288E-02	0.10565E-01	-0.12288E-02	0.16866E-04	0.14114E-02	0.92111E-02	-0.62723E-03	0.74784E-05	0.74113E-04
-5.15	0.11707E-01	-0.10855E-02	0.98765E-05	0.32433E-03	0.15944E-01	-0.19890E-02	0.18347E-04	0.11704E-02	0.10076E-01	-0.74811E-03	0.77708E-05	0.73473E-03
-5.32	0.14871E-01	-0.13257E-02	0.25084E-05	-0.13013E-04	0.12398E-01	-0.12435E-02	0.90198E-05	0.10240E-02	0.15990E-01	-0.16276E-02	0.13150E-04	0.10380E-02
-5.50	0.17672E-01	-0.16308E-02	0.31250E-05	0.61925E-03	0.13649E-01	-0.10315E-02	0.23133E-05	0.94592E-04	0.14025E-01	-0.99704E-03	0.35459E-05	0.12496E-02
-5.67	0.16719E-01	-0.10465E-02	-0.55670E-05	-0.77473E-04	0.18458E-01	-0.13979E-02	0.34573E-07	-0.72259E-05	0.13089E-01	-0.16932E-03	-0.12810E-04	0.17285E-03
-5.85	0.29296E-01	-0.24428E-02	-0.14716E-04	-0.43208E-03	0.22706E-01	-0.13343E-02	-0.12400E-04	-0.12816E-02	0.23371E-01	-0.12222E-02	-0.16222E-04	0.10031E-02
-6.02	0.33937E-01	-0.24670E-02	-0.18312E-04	0.18092E-03	0.39317E-01	-0.32252E-02	-0.16003E-04	-0.70935E-03	0.35791E-01	-0.17828E-02	-0.35404E-04	0.96633E-03
-6.20	0.51062E-01	-0.33706E-02	-0.46305E-04	-0.10764E-02	0.57131E-01	-0.41146E-02	-0.46812E-04	-0.95558E-03	0.68369E-01	-0.42832E-02	-0.67022E-04	0.74193E-03

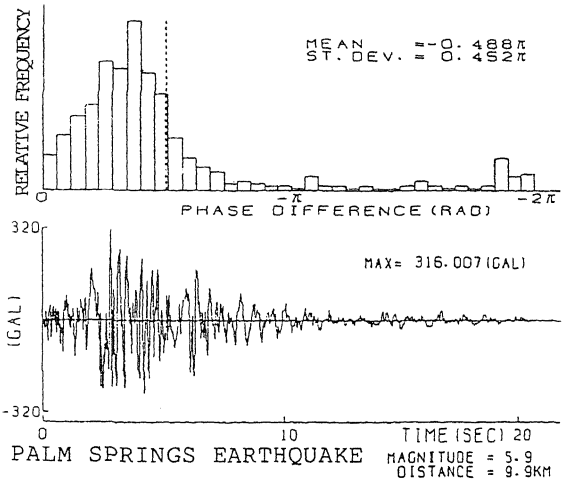

Fig. 1 The Earthquake Ground Motion and The Phase Difference Distribution

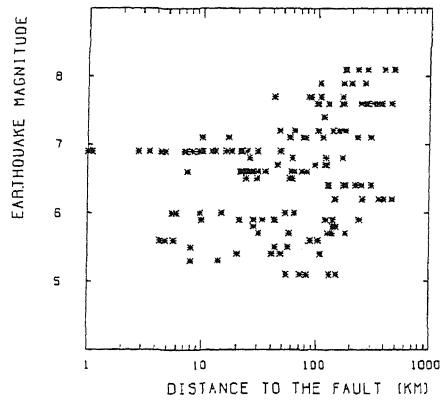

Fig. 2 Magnitudes and Distances to The Fault of The Data Base

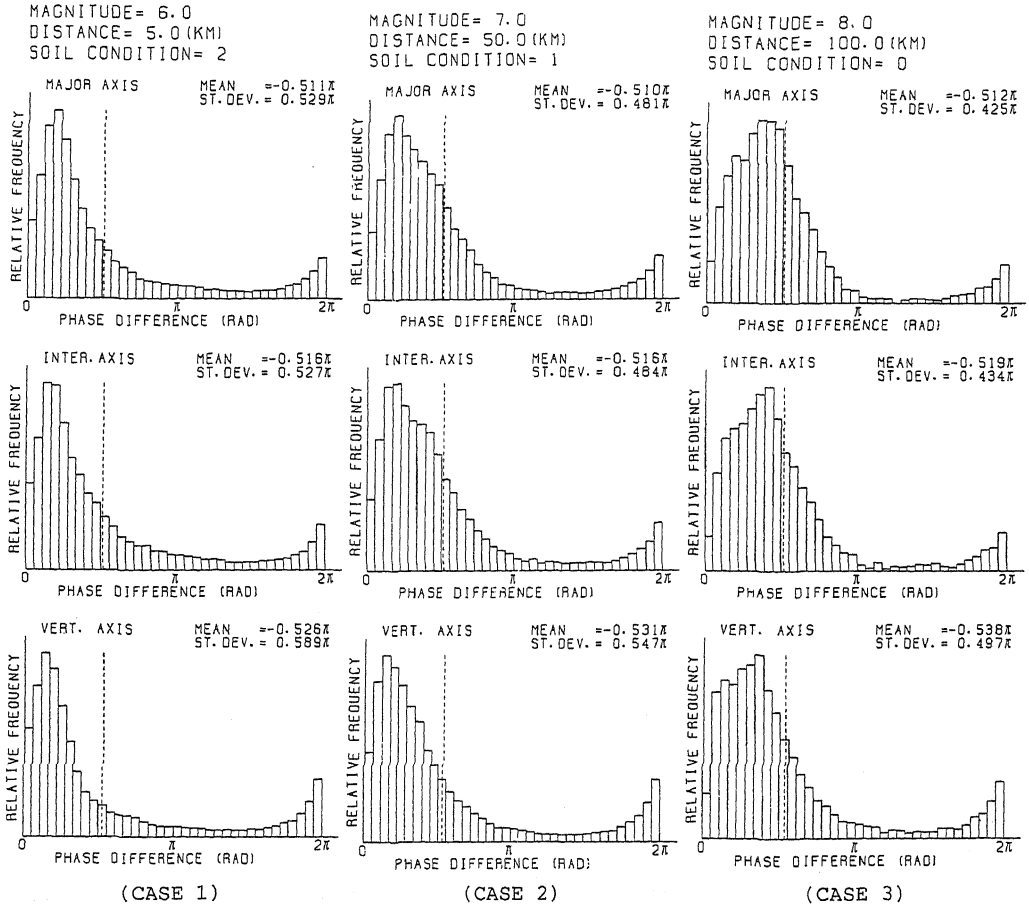

Fig. 3 Phase Difference Distributions by Regression Analysis

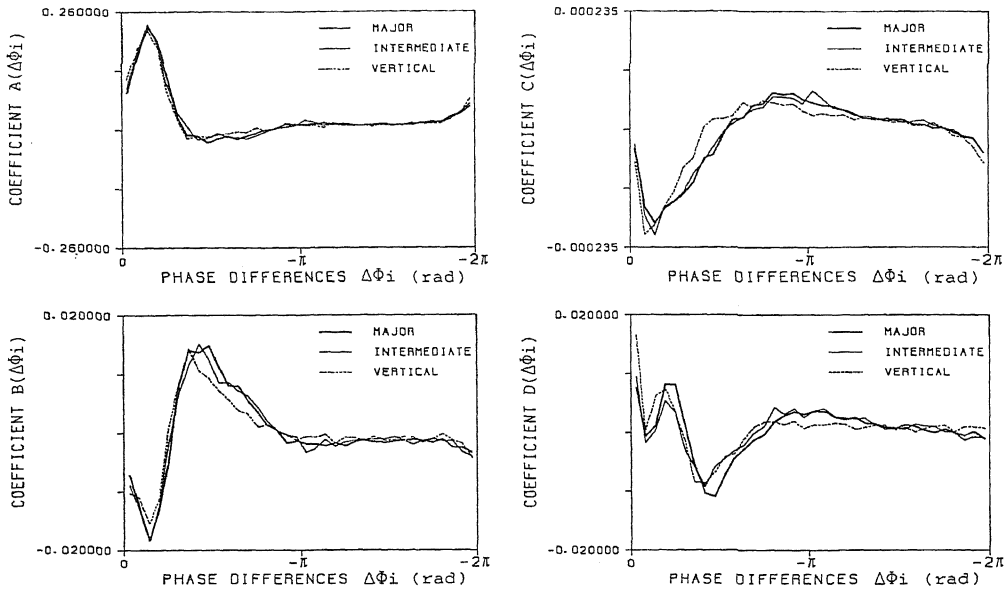

Fig. 4 Regression Coefficients

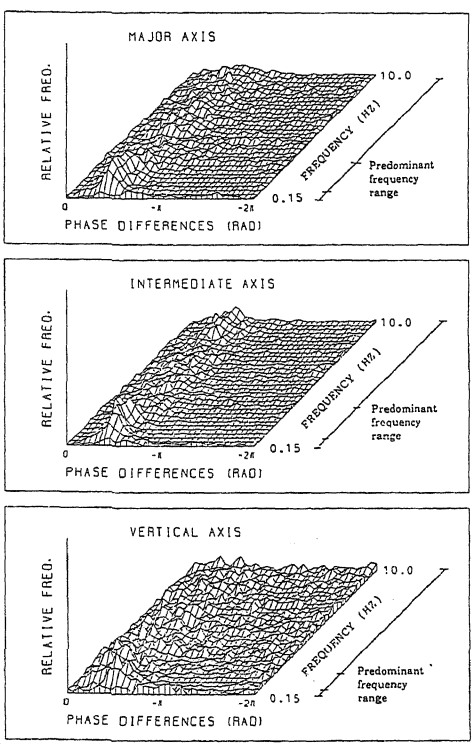

(1978 IZU-OSHIMA EARTHQUAKE)

Fig. 5 Sub-Distributions Dependent on Frequencies

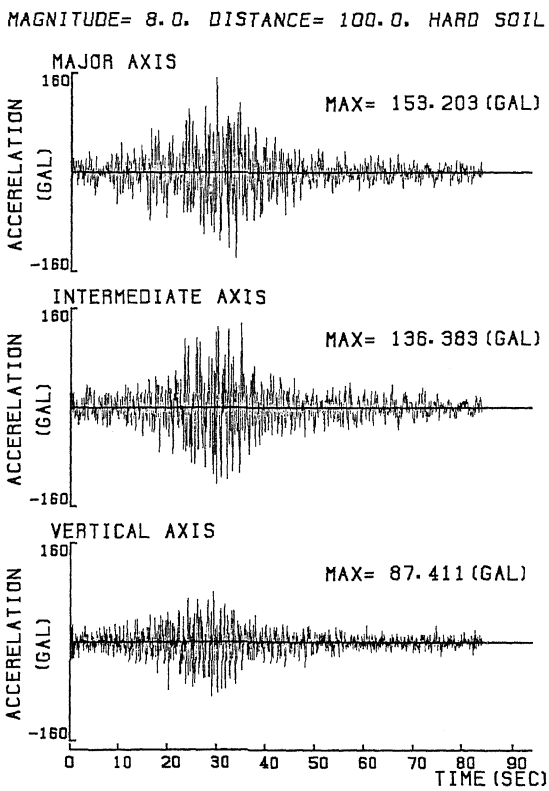

Fig. 6 Synthetic Earthquake Motions along The Principal Axes